ORIGINAL ARTICLE

A morphometric study of the human fetal heart on post-mortem 3-tesla magnetic resonance imaging

Inga Sandaite[1,5], Luc De Catte[2], Philippe Moerman[3], Marc Gewillig[4], Luigi Fedele[5], Jan Deprest[2] and Filip Claus[1]*

[1]Department of Radiology, University Hospitals Leuven, Leuven, Belgium
[2]Department of Obstetrics and Gynaecology, University Hospitals Leuven, Leuven, Belgium
[3]Department of Pathology, University Hospitals Leuven, Leuven, Belgium
[4]Department of Pediatric and Congenital Cardiology, University Hospitals Leuven, Leuven, Belgium
[5]Department of Obstetrics and Gynaecology, Fondazione Ca' Granda, Ospedale Maggiore Policlinico, Milan, Italy
*Correspondence to: Filip Claus. E-mail: filip.claus@uzleuven.be

ABSTRACT

Objective To report on the feasibility of assessing cardiac structures on post-mortem 3-tesla MRI (pmMRI) and to provide morphometric data in fetuses without cardiac abnormalities.

Methods Retrospective single center study on 3T pmMRI of 39 consecutive fetuses without cardiac abnormalities (13–38 weeks of gestation). Fetal cardiac anatomy was assessed and measurements of cardiac structures were performed on T2-weighted 3D multiplanar reconstructed images. Linear regression analysis was performed to examine changes of cardiac dimensions during gestation.

Results The four-chamber view of the fetal heart could be obtained and the measurements of cardiac chambers and ventricular walls could be performed in all 39 cases. The aorta and the pulmonary artery were visualized and their diameters were measured in 38 (97.4%) fetuses, ductus arteriosus in 32 (82%). All measurements showed strong linear correlation with gestational age. The relationship of the diameters of the pulmonary artery, aorta, and ductus arteriosus remained constant over pregnancy. All these observations are consistent with what is known from prenatal ultrasound.

Conclusions The present study proves the feasibility of visualizing normal cardiac structures on 3-tesla pmMRI in fetuses beyond 14 weeks. We provide morphometric data that may enable diagnostic evaluation of cardiac abnormalities on pmMRI. © 2013 John Wiley & Sons, Ltd.

Funding sources: JAD beneficiates from a fundamental clinical research grant of the Fonds Wetenschappelijk Onderzoek Vlaanderen (1.8.012.07.N.02). IS is beneficent of a research grant from the Klinisch Onderzoeksfonds (KOF) of the UZ Leuven.
Conflicts of interest: None declared

INTRODUCTION

Conventional autopsy represents at present the gold standard for post-mortem investigation of the fetus. The contribution of fetal and neonatal post-mortem examination to clinical practice is widely recognized and well-documented.[1–4] Despite the proven value of autopsy, the rate of post-mortem examinations of newborns and children has declined over the last three decades.[5–7] This is probably due to combination of several reasons; one of the major objections making many families declining to consent is the invasive nature of the procedure.[8]

Therefore, post-mortem magnetic resonance imaging (pmMRI) was proposed more than a decade ago as an alternative to conventional autopsy.[9,10] pmMRI theoretically provides detailed anatomic insight in a non-invasive way. One recent study showed that pmMRI is accepted by nearly all mothers.[11] Several studies showed that pmMRI is a valuable adjunct for the examination of central nervous system, whereas identifying cardiovascular anomalies seemed to be problematic.[8,9,12–16] However, in the recent years, technical advances, such as three-dimensional and high-field strength (9.4T) MRI, improved cardiac evaluation on pmMRI. With regard to structural abnormalities in small fetuses, 9.4T MRI was shown to have a good diagnostic accuracy.[17] One group reported on the diagnostic usefulness of such technique compared with low-field pmMRI in human fetuses with congenital heart disease.[18] However, only fetuses between 11 and 20 weeks were examined, because the bore diameter of the 9.4T magnets does not accommodate larger fetuses. To our knowledge, at present time, there are no studies reporting on the assessment of the normal fetal heart on pmMRI. Therefore, we aimed to document the ability of 3-tesla pmMRI to visualize relevant cardiac structures in a group of fetuses with proven normal cardiac anatomy and to provide morphometric data that could be helpful for diagnostic evaluation of cardiac abnormalities on pmMRI.

MATERIALS AND METHODS

Study population

The study protocol was approved by the local ethics committee. We retrospectively reviewed the fetal pmMRI that were performed in our center during a two and a half year period (December 2008–June 2011) after termination of pregnancy (TOP) for chromosomal or severe structural abnormalities diagnosed by detailed prenatal imaging or following intrauterine fetal death.

For the present study, only fetuses with normal cardiac anatomy were selected. Inclusion criteria were: (1) singleton pregnancies with known exact gestational age (GA) based on first trimester ultrasound (US); (2) absence of fetal congenital heart anomalies either on prenatal ultrasound or on pathological examination; (3) normal fetal growth reported on prenatal ultrasound and (4) image quality sufficient to define most of the fetal cardiac structures. We purposely excluded fetuses with abnormalities that are likely to alter cardiac dimensions or confound biometric measurements, such as congenital diaphragmatic hernia, chest anomalies in skeletal dysplasia, pulmonary hypoplasia in fetuses with renal anomalies, and fetal hydrops. Moreover, fetuses with chromosomal anomalies that are known to be associated to cardiac abnormalities were also excluded from this study. Only three fetuses were excluded because of poor image quality, two of them were 14 weeks of gestation and one 13 weeks and 5 days. Moreover, one of these fetuses was imaged on MRI 35 h after delivery.

For TOP prostaglandin induction of labor alone was used for early or midterm pregnancies. For terminations at 24 weeks or beyond, intracardiac injection of potassium chloride or injection of lidocaine hydrochloride (Linisol) and fentanyl (Fentanyl–Janssen) was used before induction of labor with prostaglandins. Fetuses were kept in the delivery ward at 4 °C until MRI was performed.

After the MRI and in case informed consent was obtained from the parents, fetuses were referred for conventional autopsy carried out by an experienced fetal pathologist according to a predesigned protocol.

Post-mortem magnetic resonance imaging

Magnetic resonance autopsy imaging (unfixed tissue) was performed on 3.0-tesla units (either Magnetom Trio, Siemens Medical Systems, Erlangen, Germany; or Achieva TX, Philips Medical Systems, Best, the Netherlands). The fetus was positioned supine and imaged with the wrist, knee, or head coil according to the size of the fetus. Small fetuses were placed in a 60 mL syringe filled with iso-osmolar solution (to increase sample size on MRI). For assessment of fetal anatomy, we used T2-weighted images, obtained using a 3D turbo spin echo (HASTE) sequence with the following parameters: TE 131 ms, TR 1000 ms, slice thickness 0.3 to 0.8 mm (according to the size of the fetus), no intersection gap, field-of-view > 200 × 200 mm. These parameters allowed acquiring images with isotropic voxel resolution, suitable for high-resolution multiplanar reconstruction (MPR). All fetuses were imaged according to a predesigned full body MRI protocol, with a maximum acquisition time of 40 min, independently from GA.

Magnetic resonance imaging analysis

The fetal heart analysis was performed offline on MPR images using Picture Archiving and Communication System (PACS, Agfa-Gevaert N.V., Mortsel, Belgium). To investigate different cardiac structures, we generated multiple views corresponding to those prenatally obtained by ultrasound: upper abdomen view, four-chamber view, five-chamber view, as well as main pulmonary artery (PA) with bifurcation into left and right PAs, and three-vessel and trachea view. In addition, by using multiplanar imaging, we had a freedom to recreate numerous images not only from the standard axial, sagittal, and coronal planes, but also from different oblique planes.

Each heart was assessed by a sequential segmental approach as suggested by Carvalho *et al*, *2005*.[19] First, visceroatrial situs, cardiac position, size, and axis were established. Second, number, arrangement, and relative size of the cardiac chambers were analyzed. Moreover, position of the atrioventricular valves, as well as continuity of the interventricular septum, was assessed. The inflow veins (superior and inferior vena cava [SVC/IVC], pulmonary veins) and the outflow vessels (aorta [Ao], PA, ductus arteriosus [DA]) were evaluated with emphasis on their relative size, origin, and course. In addition, the presence of the aortic and pulmonary valves was determined.

Measurements

All the measurements of fetal cardiac structures were performed on MPR images by a single operator. First, on a transverse plane of the fetal chest at the four-chamber view, cardiac and thoracic circumferences were measured (Figure 1). They were expressed as a cardiothoracic (C/T) circumference ratio, by dividing cardiac circumference by thoracic circumference. Further, on the same four-chamber view, transverse internal diameters of ventricular and atrial cavities, as well as the thickness of ventricular walls and interventricular septum, were assessed (Figure 2). The transverse internal diameter of each atrium was measured at the level where the diameter was largest, from the lateral wall to the septum atrium primum. The transverse internal diameter

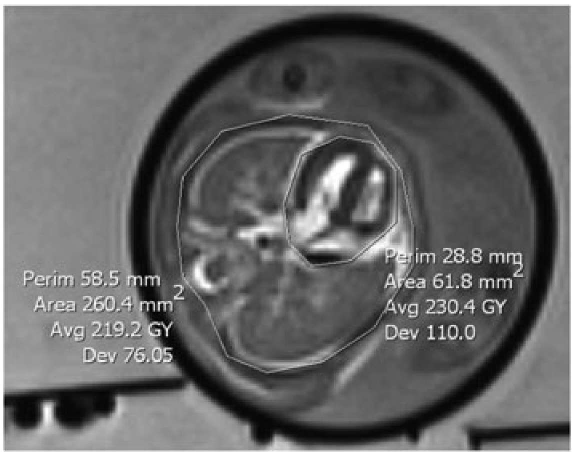

Figure 1 MPR PMMR image (transverse plane) in a 13 weeks and 2 days fetus with encephalocele showing measurements of cardiac and thoracic circumferences at four-chamber view. The fetus is scanned in a 60 mL syringe filled with iso-osmolar solution

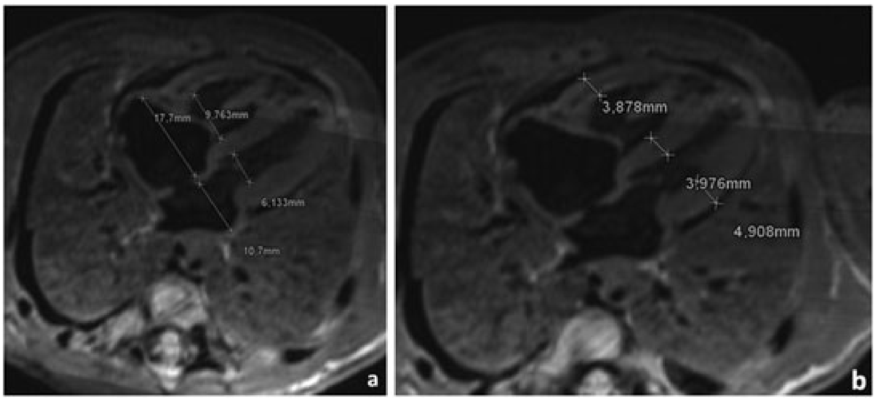

Figure 2 MPR PMMR image (transverse plane) demonstrating four-chamber view in a 33 week fetus with meningocele. The arrows indicate the points for measurements of (a) cardiac cavities (atria and ventricles) as well as (b) the thickness of ventricular walls and interventricular septum

of each ventricle (endocardial-to-endocardial) was determined just below the atrioventricular valve. The thickness of the ventricular wall (endocardial-to-epicardial surface) and the ventricular septum were measured just below the atrioventricular valves. Internal diameters of Ao, PA, DA, and SVC were assessed on multiple views. The diameter of each vessel was measured in different planes (multiplanar view with three orthogonal planes), and the mean of two measurements was taken for further analysis (Figure 3). The diameters of ascending Ao, as well as PA, were assessed above the aortic and pulmonary valves at the level of the sinotubular junction. Moreover, the ratio of the diameter of the PA to the diameter of the ascending Ao (PA/Ao ratio) was calculated. The diameter of the descending Ao was taken just below the entrance of the DA. Further, the diameter of the DA was obtained at its middle, half the distance between its union with the Ao and the PA (Figure 3). The measurement of the SVC was carried out at its entry into the right atrium. In most cases, on the transverse view, the IVC appears as an oval-shaped structure slightly compressed antero-posteriorly. Assuming that it was more circular *in vivo*, the diameter of the IVC was calculated from the circumference (for the purpose of graphic presentation). The latter was taken on the axial view where the IVC enters into the right atrium (Figure 4b). In all cases, measurements were performed only when the image quality was good enough to allow clear definition of the structures.

Statistical analysis

Statistical analysis was performed using Excel 2010 (Microsoft Corp., Remond Wash., USA). Linear regression analysis was used to determine the relationship between the measurements of different cardiac structures and the GA.

RESULTS

Out of 160 pmMRI examinations, 39 matched the inclusion and exclusion criteria. The median GA was 24 weeks (range 13 w 2 d–38 w 6 d). Of the 39 fetuses, 17 were female fetuses, and 22 were male fetuses. Thirty-seven fetuses underwent TOP, and two were intrauterine fetal death. The medical indications for the TOP are displayed in Table 1. Feticide was performed in TOP in 26 cases. A prostaglandin induction of labor was performed in all cases. Among the 39 fetuses, four had no conventional autopsy (10.3%): three cases were terminated because of a genetic disorder, and in one, a cytomegalovirus fetopathy was present. pmMRI was performed within the interval of 1 h 10 min to 20 h 30 min (median 6 h 30 min) after delivery of the fetus. The median isotropic voxel size was 0.5 mm (range 0.3–0.8 mm).

A four-chamber view could be obtained, and the heart and the thoracic circumferences were measured in all 39 cases (Appendix 1). The cardiothoracic ratio was fairly constant throughout gestation with a median of 51% (range 46–57%) (Figure 5). The widths of the cardiac chambers and the

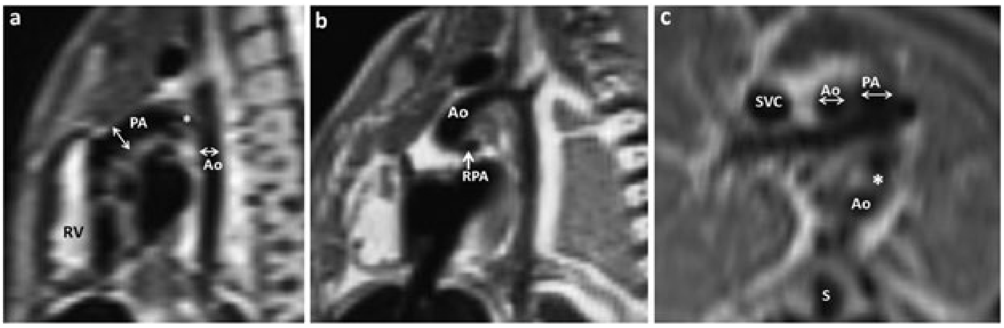

Figure 3 MPR PMMR image on sagittal/oblique (a, b) and transverse (c) planes of 18 weeks fetus with segmental spinal dysgenesis. (a) long-axis view of the right ventricle (RV); (b) long-axis view of the aortic arch; (c) three-vessel view. Arrows indicate the measurements of the diameters of aorta (Ao) and pulmonary artery (PA). Ductus arteriosus (asterix) connects the PA to the Ao. RPA right pulmonary artery; SVC superior vena cava; S spine

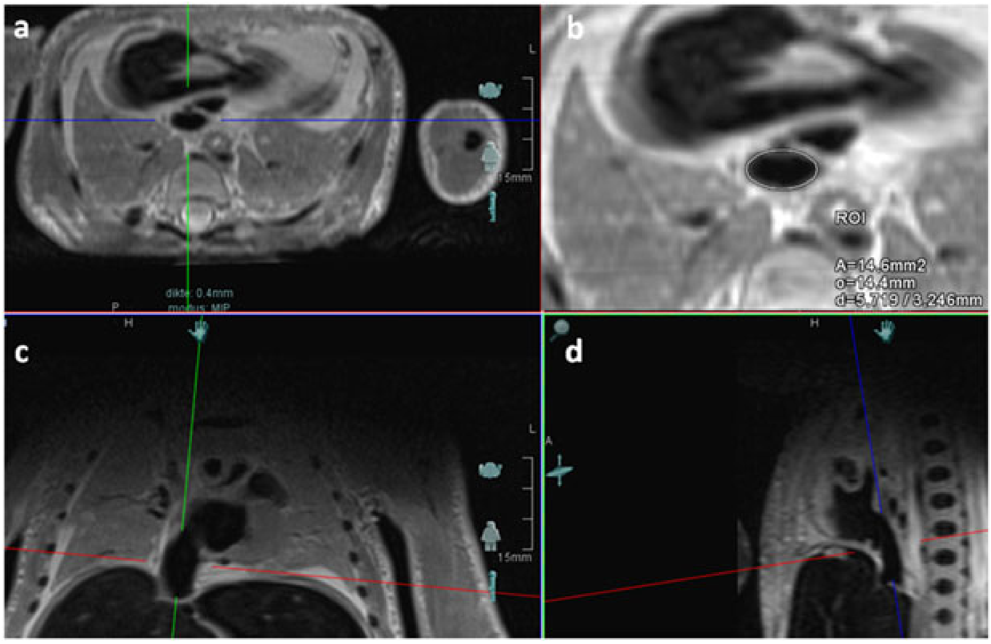

Figure 4 MPR PMMR images demonstrates inferior vena cava (IVC) on (a, b) transverse, (c) coronal, and (d) sagittal planes in a 24-week fetus with genetic disorder. (b) IVC appears as an oval shaped structure slightly compressed antero-posteriorly. (b) measurement of the perimeter of IVC at her entry into the right atrium

ventricular wall thickness, as well as of the interventricular septum, were successfully assessed in all cases. The diameter of the left atrium ranged between 2.0 and 12.8 mm (median 7.6 mm), being slightly smaller than the right atrium (range 2.0–19.7 mm, median 10.0 mm). Both ventricles were almost equal in size ranging between 1.0 and 12.3 mm, with the median value of 4.8 mm for the left ventricle and 4.7 mm for the right ventricle. The median value of the ventricular wall thickness was 3.8 mm for the left ventricle (range 1.2–6.4 mm), 3.5 mm for the right ventricle (range 1.2–6.2 mm), and 3.1 mm for the interventricular septum (range 1.1–5.5 mm). The great arteries (Ao and PA) were visualized and measured in 38 cases (97%). The only one where it was not possible was a fetus of 13 weeks and 2 days of gestation. The DA was successfully assessed in 32 cases (82%) (Appendix 2). The PA (median 3.9 mm, range 1.3–6.5 mm) had the largest diameter throughout gestation, whereas the ascending Ao (median 3.3 mm, range 1.1–5.6 mm) followed the same growth curve but was slightly smaller than PA, whereas the DA (median 1.3 mm, range 0.6–3.0 mm) had the smallest diameter (Figure 6). The PA/Ao ratio was calculated in 38 cases and plotted against GA (range 0.85–1.58, median 1.16) (Figure 6). SVC and IVC have been visualized and measured in all 39 fetuses. The pulmonary veins were not seen in one fetus of 13 weeks of gestation. The presence of the aortic and pulmonary valves was noted respectively in 32 (82%) and in 33 (84.6%) cases. On four-chamber view, the insertion of the tricuspid valve and the mitral valve was visualized in 26 (66.7%) and 30 (76.9%) cases, respectively. Five of these fetuses, in which both atrioventricular valves could not have been assessed on pmMRI, were fetuses below 18 weeks of gestation. In the remaining fetuses at different GA, fluid levels due to post-mortem blood sedimentation were observed.

A significant correlation between GA and the dimensions of cardiac structures was found, with linear growth over time (Appendix 3[a,b]).

DISCUSSION

Herein, we demonstrate the feasibility of visualizing fetal cardiac structures on 3-tesla pmMRI. With sufficient resolution, normal cardiac structures can be discriminated and measured as early as 14 weeks of gestation.

We report on the assessment of the normal heart on 3-tesla pmMRI in fetuses between 13 and 38 weeks of gestation. In our study, we used 3D data sets with the slice thickness that ranged between 0.3 and 0.8 mm. As a result, we obtained isometric voxel sizes for MPR in nearly all cases, clearly improving the MPR image quality and resulting in better visualization of the cardiac structures. As previous post-mortem studies have primarily used low field strengths and 2D data sets,[20–22] this could explain the difficulty to assess the fetal heart. The use of higher field strength and isotropic 3D sequences optimizes the image quality for multiplanar evaluation of the cardiac structures.

One recent study compared the diagnostic utility of 1.5T, 3T, and 9.4T MRI in fetuses at or under 20 weeks of gestation.[18] The authors concluded that only by using a 9.4T MRI fetal cardiac structures could be visualized irrespective of GA. The former study mainly focused on fetuses with congenital heart disease. However, to our knowledge, to date, no dedicated studies are available on cardiac evaluation on pmMRI in fetuses without cardiac pathologies. Moreover, our study provides biometric data of cardiac structures on pmMRI over a wide GA range. Our results show that all cardiac dimensions have a strong linear correlation with GA as previously

Table 1 Medical indications for termination for pregnancy in 37 fetuses

Type of anomaly	Number of cases
Intrauterine infection:	
Cytomegalovirus infection	11
Toxoplasmosis	1
Neural tube defects	
Meningocele	2
Encephalocele	1
Lumbosacral spina bifida	2
Other nervous system anomalies:	
Callosal agenesis (one case associated with pes equinus)	2
Intracranial bleeding	1
Hydrocephaly (post-hemorrhagic; by third ventricular obstruction)	2
Rhombencephalosynapsis	1
Megalencephaly polymicrogyria, and hydrocephalus syndrome	1
Spinal dysgenesis	1
Fetal hypokinesia (migration disorder; suspect of valproic acid embryopathy)	2
Distal arthrogryposis	2
Cloacal dysgenesis	1
Harlequin ichthyosis	1
Amniotic band syndrome	1
Microphthalmia and ventriculomegaly	1
Genetic disorders:	
Mucoviscidosis (=cystic fibrosis)	1
Unbalanced translocation 5 and 6 (palatoschisis/cleft lip on US);	1
PGRN mutation, known to be associated with frontotemporal dimension	1
PROM at 18 weeks of gestation	1

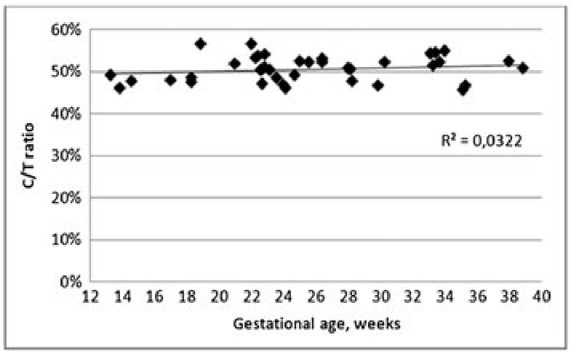

Figure 5 Cardiothoracic (C/T) ratio throughout gestation in 39 fetuses without cardiac abnormalities

described for measures by prenatal ultrasound[23] and post-natally on conventional autopsy.[24,25] Interestingly, the absolute values do not match perfectly; they seem to be slightly lower than those of reference ranges derived from 2D fetal echocardiography.[23,26,27] Prenatal sonographic measurements are taken at a definite point in the cardiac cycle (end-diastole), when the chamber size and vessel diameter are at their maximal size, and the ventricular wall dimensions are the thinnest. Moreover, on prenatal ultrasound, some authors measure the diameters of the great vessels at the level of the valve,[23,26] what also could result in slightly higher values. Because in some cases on PMMR images, the valve is not clearly visible, we chose to measure the diameters of Ao and PA just above the assumed valvular level. Even reference charts derived from morphological studies are often unreliable for *in vivo* measurements.[24,28]

Although individual values for the measurement of different cardiac structures seem to differ from those reported in the literature, the C/T ratio was concordant with prenatal findings,[29] about 50%. Wong *et al*. (*2007*)[30] assessed PA/Ao ratio at the level of three-vessel view in a group of 966 fetuses between 16–24 weeks of gestation, and it was comparable to the one in our study (1.14 and 1.16, respectively), highlighting that although post-mortem changes might slightly alter the dimensions of cardiac structures, the relationship between the dimensions is maintained.

Two major strengths of our study are (1) the short time delay between delivery and pmMRI and (2) the use of 3D sequences with isovolumetric voxel size on a 3T MRI. This allowed us to acquire good quality images for MPR and provided us with an unlimited choice of image orientation to view the cardiac structures in any desirable plane. Moreover, as 3T MR units have no limitations regarding the size of the fetus and are clinically more readily available, we could include in our study fetuses from 13 weeks of gestation up to term. As shown by other groups, the use of 9.4-tesla MRI provides an even better tissue contrast and spatial resolution for evaluating the fetus up to 20 weeks of gestation.[17,18] Although the assessment of actual diagnostic value of this technique was beyond the aim of this study, we showed that the main cardiac structures can be identified on 3T pmMRI in fetuses beyond 14 weeks. Moreover, this technique allows examination of the fetal heart *in situ*, where connections with other structures are maintained and can easily be assessed. Furthermore, very small structures can be assessed.

Our study has several limitations. First, although we focused on pregnancies terminated for various non-cardiac abnormalities, they may not be fully representative for a normal healthy fetal population. Therefore, only fetuses with anomalies not interfering with the cardiac anatomical development and function and with documented normal growth were included. The fetuses in this study group were not homogeneously distributed throughout gestation. We are aware that accurate morphometry may prove more difficult in non-preselected cases or fetuses with cardiac pathology, but the aim of this study was to investigate the ability of pmMRI to visualize and measure the structures of the normal fetal heart. Further studies in fetuses with cardiac or chest abnormalities are necessary to validate the usefulness of the provided normal reference data. Second, as one of the objectives of the study was to provide reference values for cardiac measurements, we limited our population to cases

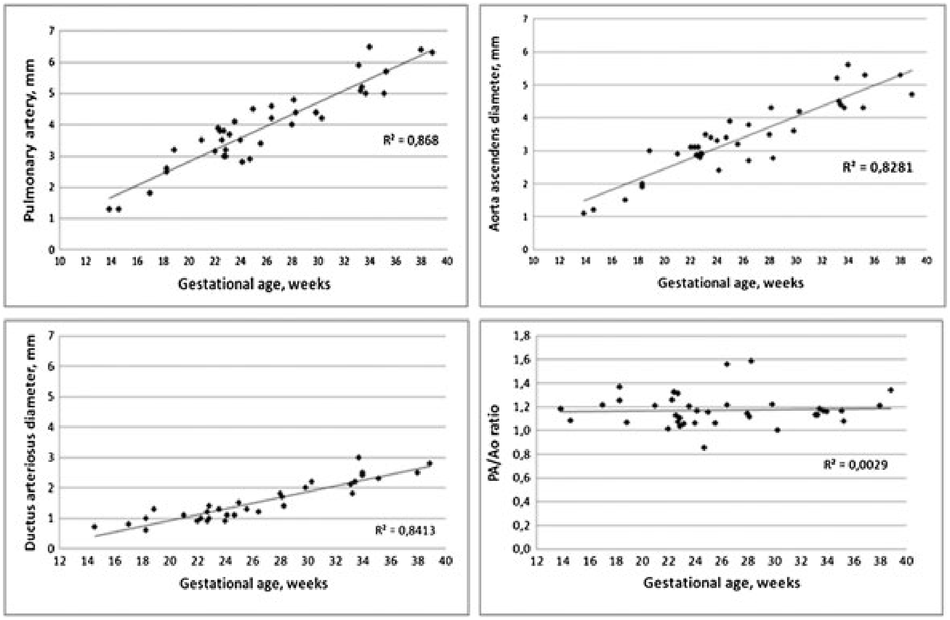

Figure 6 Scatter-plots of pulmonary artery (left top image), aorta (right top image), and ductus arteriosus (left bottom image) demonstrating their growth (diameters measured on MPR 3T PMMR images) throughout gestation in fetuses without cardiac abnormalities. Pulmonary artery/aorta (PA/Ao) ratio throughout gestation (right bottom image)

with good quality MR images (based on a subjective visual assessment). Among all cases that met the other inclusion criteria, only three cases had an unacceptable image quality. All three of them had a GA less than 15 weeks. At last, post-mortem changes related to cessation of circulation and post-mortem muscle contractions might limit the interpretation and influence the correct biometry on PMMR images. As in our case, we experienced difficulties to visualize the cardiac valves and the continuity of the DA due to blood sedimentation in cardiac chambers. Post-mortem contraction of the fetal heart muscle might alter cardiac dimensions, resulting in smaller ventricle cavities and thicker ventricular walls. In the total post-mortem population of 160 fetuses, cardiac contraction was observed on pmMRI in only two cases. Both of them had a GA of 24 weeks and were not included in the study population, on the basis of the inclusion criteria. The measurements of the ventricular walls and the ventricular cavities for these two cases were clear outliers on the presented cardiac reference graphs.

To conclude, cardiac pmMRI evaluation using 3T equipment allows the demonstration of normal cardiac anatomy and biometry in fetuses beyond 14 weeks. The presented data could serve as references for the detection of cardiac pathology on post-mortem MR images.

WHAT'S ALREADY KNOWN ABOUT THIS TOPIC?

- Post-mortem fetal magnetic resonance imaging (pmMRI) is a valuable addition or alternative for conventional autopsy examination. Studies investigating the normal fetal anatomy on pmMRI are sparse.

WHAT DOES THIS STUDY ADD?

- This study (1) comprehensively describes the methodology of the assessment of the normal fetal heart on pmMRI and (2) provides morphometric data helpful for the diagnostic evaluation of cardiac abnormalities on pmMRI.

REFERENCES

1. Burton JL, Underwood J. Clinical, educational, and epidemiological value of autopsy. Lancet 2007;369(9571):1471–80.
2. Faye-Petersen OM, Guinn DA, Wenstrom KD. Value of perinatal autopsy. Obstet Gynecol 1999;94(6):915–20.
3. Cartlidge PH, Dawson AT, Stewart JH, Vujanic GM. Value and quality of perinatal and infant postmortem examinations: cohort analysis of 400 consecutive deaths. BMJ 1995;310(6973):155–8.
4. Porter HJ and Keeling JW. Value of perinatal necropsy examination. J Clin Pathol 1987;40(2):180–4.
5. Adappa R, Paranjothy S, Roberts Z, Cartlidge PHT. Perinatal and infant autopsy. Arch Dis Child Fetal Neonatal 2007;Ed 92:F49–50.
6. Khong TY, Tanner AR. Foetal and neonatal autopsy rates and use of tissue for research: the influence of 'organ retention' controversy and new consent process. J Paediatr Child Health 2006;42(6):366–9.
7. Brodlie M, Laing IA, Keeling JW, *et al*. Ten years of neonatal autopsies in tertiary referral centre: retrospective study. BMJ 2002;324:761–3.
8. Griffiths PD, Paley MN, Whitby EH. Post-mortem MRI as an adjunct to fetal or neonatal autopsy. Lancet 2005;365(9466):1271–3.
9. Brookes JA, Hall-Craggs MA, Sams VR, Lees WR. Non-invasive perinatal necropsy by magnetic resonance imaging. Lancet 1996;348 (9035):1139–41.
10. Ros PR, Li KC, Vo P, Baer H, Staab EV. Pre-autopsy magnetic resonance imaging: initial experience. Magn Reson Imaging 1990;8(3):303–8.
11. Cannie M, Votino C, Moerman P, *et al*. Acceptance, reliability and confidence of diagnosis of fetal and neonatal virtuopsy compared with conventional autopsy: a prospective study. Ultrasound Obstet Gynecol 2012;39(6):659–65. doi: 10.1002/uog.10079. Epub 2012 May 22.
12. Breeze AC, Jessop FA, Set PA, *et al*. Minimally-invasive fetal autopsy using magnetic resonance imaging and percutaneous organ biopsies:

clinical value and comparison to conventional autopsy. Ultrasound Obstet Gynecol 2011;37(3):317–23. doi: 10.1002/uog.8844.
13. Thayyil S, Chandrasekaran M, Chitty LS, *et al*. Diagnostic accuracy of post-mortem magnetic resonance imaging in fetuses, children and adults: a systematic review. Eur J Radiol 2010;75(1):e142–8. Epub 2009 Nov 11. Review.
14. Huisman TA. Magnetic resonance imaging: an alternative to autopsy in neonatal death? Semin Neonatol 2004;9(4):347–53.
15. Griffiths PD, Variend D, Evans M, *et al*. Postmortem MR imaging of the fetal and stillborn central nervous system. AJNR Am J Neuroradiol 2003;24(1):22–7.
16. Woodward PJ, Sohaey R, Harris DP, *et al*. Postmortem fetal MR imaging: comparison with findings at autopsy. AJR Am J Roentgenol 1997;168(1):41–6.
17. Thayyil S, Cleary JO, Sebire NJ, *et al*. Post-mortem examination of human fetuses: a comparison of whole-body high-field MRI at 9.4 T with conventional MRI and invasive autopsy. Lancet 2009;374(9688):467–75.
18. Votino C, Jani J, Verhoye M, *et al*. Postmortem examination of human fetal hearts at or below 20 weeks' gestation: a comparison of high-field MRI at 9.4 T with lower-field MRI magnets and stereomicroscopic autopsy. Ultrasound Obstet Gynecol 2012;40:437–44.
19. Carvalho JS, Ho SY, Shinebourne EA. Sequential segmental analysis in complex fetal cardiac abnormalities: a logical approach to diagnosis. Ultrasound Obstet Gynecol 2005;26(2):105–11.
20. Huisman TA, Wisser J, Stallmach T, *et al*. MR autopsy in fetuses. Fetal Diagn Ther 2002;17(1):58–64.
21. Alderliesten ME, Peringa J, van der Hulst VP, *et al*. Perinatal mortality: clinical value of postmortem magnetic resonance imaging compared with autopsy in routine obstetric practice. BJOG 2003;110(4):378–82.
22. Breeze AC, Cross JJ, Hackett GA, *et al*. Use of a confidence scale in reporting postmortem fetal magnetic resonance imaging. Ultrasound Obstet Gynecol 2006;28:918–24.
23. Shapiro I, Degani S, Leibovitz Z, *et al*. Fetal cardiac measurements derived by transvaginal and transabdominal cross-sectional echocardiography from 14 weeks of gestation to term. Ultrasound Obstet Gynecol 1998;12:404–18.
24. Ursell PC, Byrne JM, Fears TR, *et al*. Growth of the great vessels in the normal human fetus and in the fetus with cardiac defects. Circulation 1991;84:2028–33.
25. Castillo EH, Arteaga-Martínez M, García-Peláez I, *et al*. Morphometric study of the human fetal heart. I. Arterial segment. Clin Anat 2005; 18(4):260–8.
26. Lee W, Riggs T, Amula V, *et al*. Fetal echocardiography: z-score reference ranges for a large patient population. Ultrasound Obstet Gynecol 2010;35(1):28–34.
27. Schneider C, McCrindle BW, Carvalho JS, *et al*. Development of Z-scores for fetal cardiac dimensions from echocardiography. Ultrasound Obstet Gynecol 2005;26(6):599–605.
28. Alvarez L, Aránega A, Saucedo R, *et al*. Morphometric data on the arterial duct in the human fetal heart. Int J Cardiol 1991;31(3):337–44.
29. Paladini D, Chita SK, Allan LD. Prenatal measurement of cardiothoracic ratio in evaluation of heart disease. Arch Dis Child 1990;65:20–3.
30. Wong SF, Ward C, Lee-Tannock A, *et al*. Pulmonary artery/aorta ratio in simple screening for fetal outflow tract abnormalities during the second trimester. Ultrasound Obstet Gynecol 2007;30(3):275–80.

APPENDIX 1

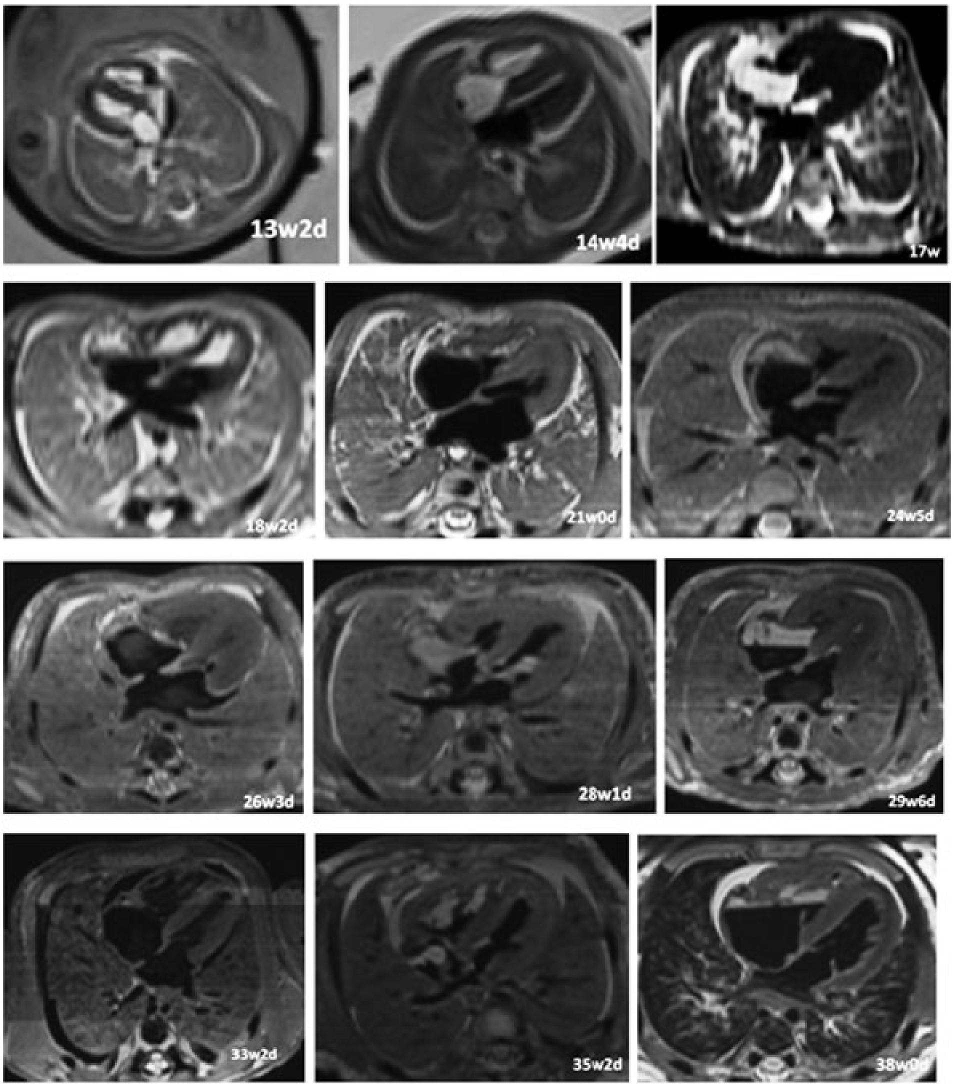

APPENDIX 2

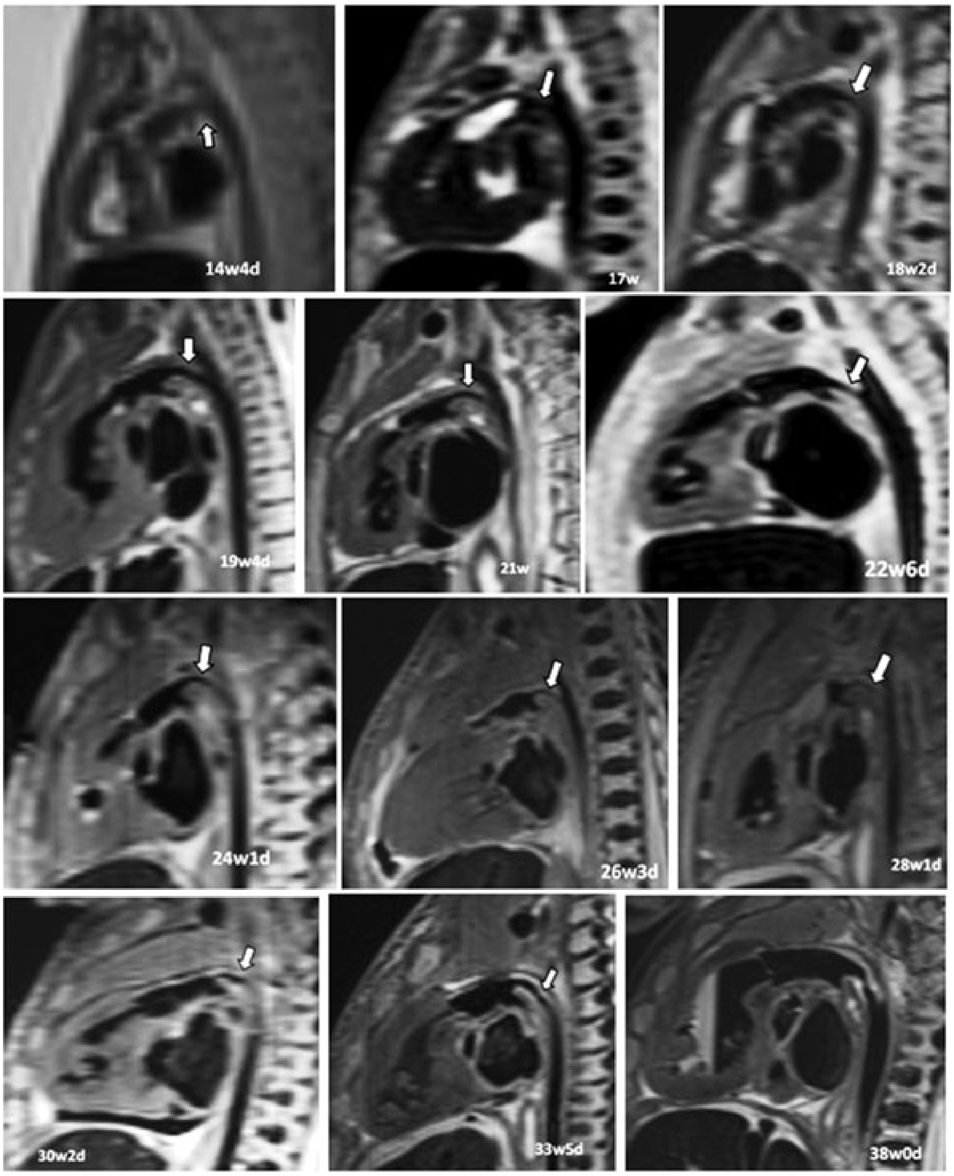
14w4d
17w
18w2d
19w4d
21w
22w6d
24w1d
26w3d
28w1d
30w2d
33w5d
38w0d

APPENDIX 3a

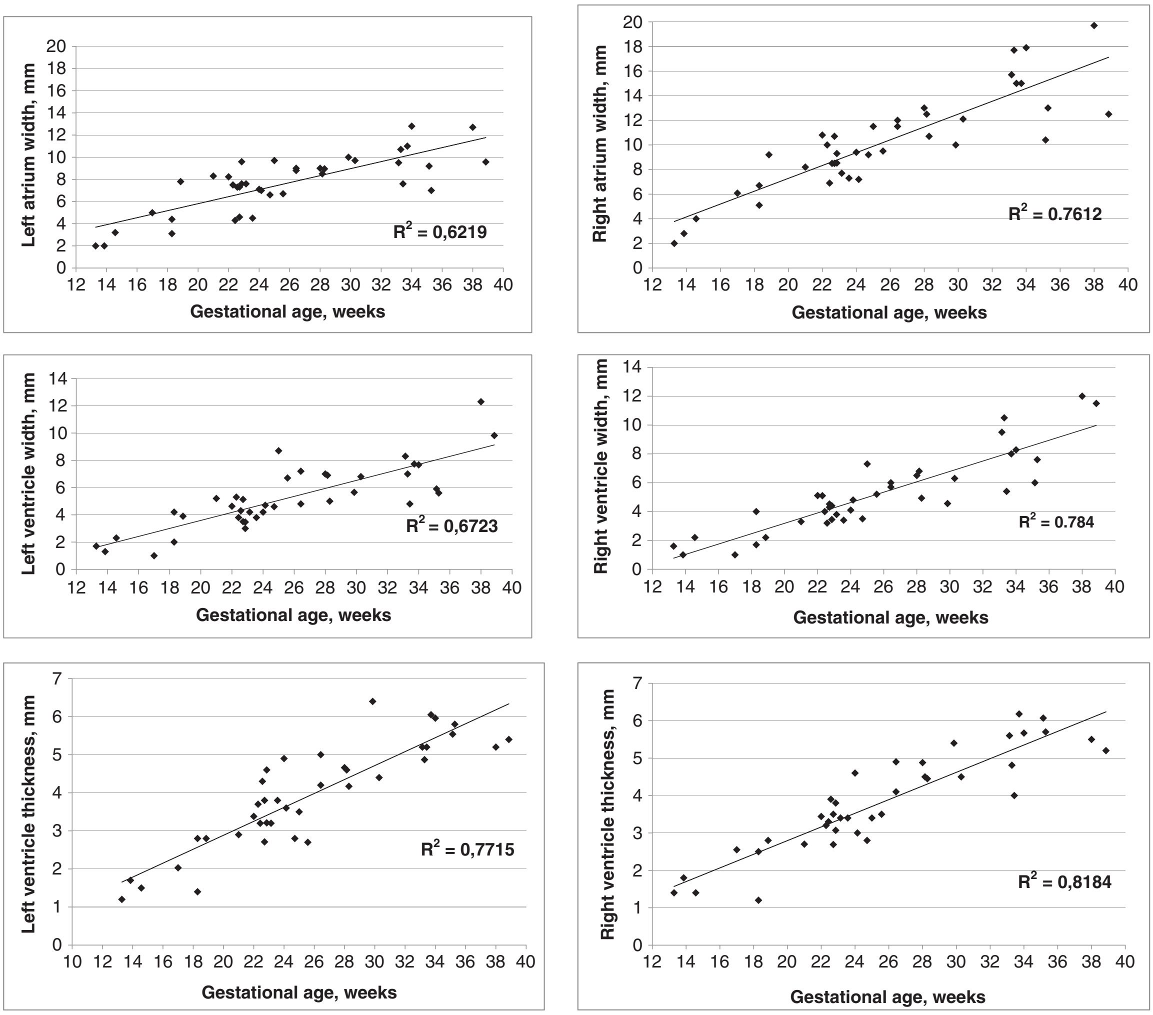
Left atrium width, mm
Gestational age, weeks
R² = 0,6219
Right atrium width, mm
Gestational age, weeks
R² = 0.7612
Left ventricle width, mm
Gestational age, weeks
R² = 0,6723
Right ventricle width, mm
Gestational age, weeks
R² = 0.784
Left ventricle thickness, mm
Gestational age, weeks
R² = 0,7715
Right ventricle thickness, mm
Gestational age, weeks
R² = 0,8184

APPENDIX 3b

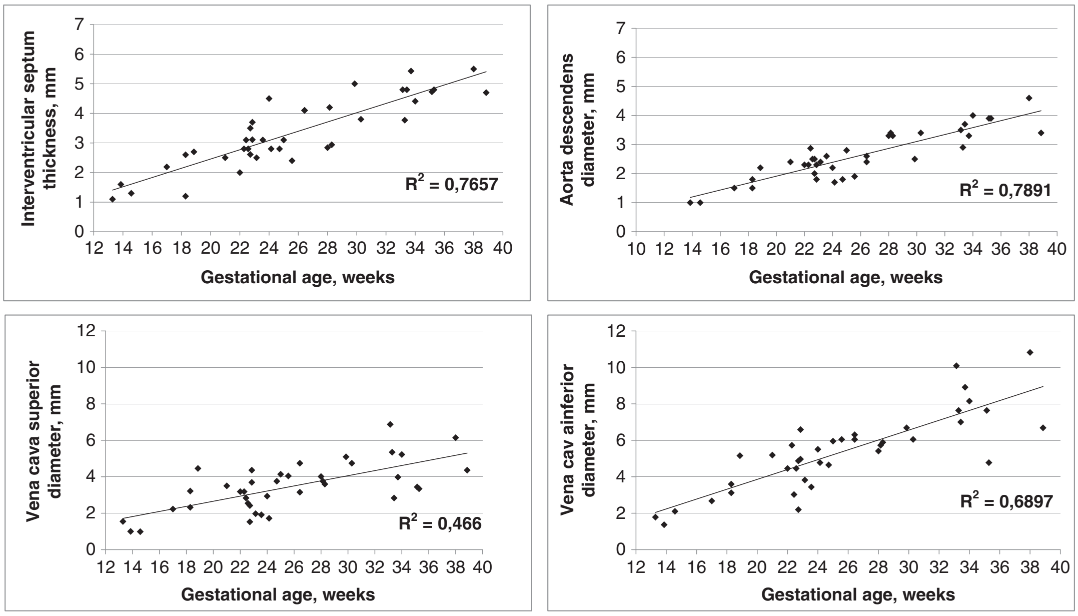
Interventricular septum thickness, mm
Gestational age, weeks
R^2 = 0,7657
Aorta descendens diameter, mm
Gestational age, weeks
R^2 = 0,7891
Vena cava superior diameter, mm
Gestational age, weeks
R^2 = 0,466
Vena cav ainferior diameter, mm
Gestational age, weeks
R^2 = 0,6897